

Strong Coupling and Double Gap Density of States in Superconducting MgB_2

F. Giubileo[†], D. Roditchev, W. Sacks, R. Lamy and J. Klein

Groupe de Physique des Solides, Universités Paris 7 et Paris 6,

Unité Mixte de Recherche C.N.R.S. (UMR 75 88), 2 Place Jussieu, 75251 Paris Cedex 5, France

[†]*Physics Department and INFM Unit, University of Salerno, via S. Allende, 84081 Baronissi (SA), Italy*

(November 7, 2018)

Using scanning tunneling spectroscopy at $T = 4.2$ K, we perform simultaneously the topographic imaging and the quasiparticle density of states (DOS) mapping in granular MgB_2 . We observe a new type of spectrum, showing a pronounced double gap, with the magnitudes of $\Delta_S = 3.9$ meV and $\Delta_L = 7.5$ meV, i.e. well below and well above the BCS limit. The largest gap value gives the ratio $2\Delta_L/k_B T_c = 4.5$, which implies strong electron-phonon coupling. Other superconducting regions are found to have a characteristic BCS-shaped DOS. However, the variation of the spectral shape and lower gap widths, from 2.0 meV to 6.5 meV, indicate the importance of surface inhomogeneity and proximity effects in previously published tunneling data. Our finding gives no evidence for any important gap anisotropy. Instead, it strongly supports the multiple gap scenario in MgB_2 in the clean limit, and the single gap scenario in the dirty limit.

PACS numbers: 74.20.-z, 74.50.+r, 74.70.Ad

Since its announcement by Nagamatsu *et al.* in January 2001 [1], the discovery of superconductivity in the simple metallic compound MgB_2 has stimulated a great effort in the field. A very high critical temperature $T_C \simeq 39$ K, well above the values reported for all other conventional superconductors, and quite simple binary structure, make this material a good candidate for technological applications. At the same time this unusually high T_C opens a new fascinating question about the electronic structure and pairing mechanism involved.

Numerous experimental reports confirm that MgB_2 is a BCS-type phonon-mediated superconductor. A significant boron isotope effect ($\alpha \simeq 0.26$) was observed in both magnetization and specific heat measurements [2]. Measurements on nuclear spin-lattice relaxation rate in the ^{11}B NMR study by Kotegawa *et al.* [3] have shown the existence of an s-wave superconducting state with a large isotropic gap ($2\Delta/k_B T_C \simeq 5$) well above the weak-coupling BCS value of 3.52. The strong coupling scenario could be explained considering the high phonon frequencies ($\omega \simeq 700$ K) in MgB_2 due to the light boron mass [4]. To complicate the picture, it has been shown theoretically that MgB_2 has a particular band structure in which both two- and three-dimensional bands are present and that, in the clean limit, could even give rise to a multiple gap superconductivity [5].

The direct measurement of the superconducting DOS of MgB_2 is urgently needed. Photoemission experiments have already been performed [6,7] but are, unfortunately, limited by energy resolution. Details of the magnitude and symmetry of the superconducting gap can be obtained with tunneling spectroscopy (TS), giving directly the quasiparticle DOS with an energy resolution of a few kT. If the full scanning TS (STS) is performed, the spatial mapping of the local DOS is possible. It has also proved useful in the case of inhomogeneous systems [8]. Finally, in the tunneling conductance, spectral features

found above the gap allow a self-consistent analysis of the electron-phonon interaction [9].

Unfortunately, the published tunneling spectra clearly diverge [10–14] and no STS data have yet been presented. While the shapes of the spectra indicate an isotropic gap for the pairing symmetry, the gap widths are quite different, all being too small to be realistic for the bulk MgB_2 . Moreover, in [11] the spectra were found exceedingly smeared. To explain these different results, even a very sophisticated symmetry was suggested for an anisotropic order parameter [15]. In this series tunneling experiments [10–14] no evidence whatever for a multiple (or double) gap scenario was shown. Consequently, an important uncertainty exists in establishing the shape of the quasiparticle DOS and the gap magnitude pertinent to the bulk superconductivity.

In this Letter we show that the complete STS, even on the small scale of a few hundred nanometers, allows one to interpret the wide variation in the previous tunneling data. The measurements were performed on MgB_2 powder ($T_C = 38.7$ K), which was glued to the sample holder by silver paint and mechanically etched Pt/Ir wires were used as STM tips. Measured locally, the conductance spectra reveal a distinct double gap structure as shown in Fig.1. These show little or no smearing other than thermal broadening at 4.2 K. As we shall argue, this double gap is an intrinsic property of MgB_2 and not a proximity effect [16].

The tunneling conductance in Fig.1 is also characterized by a very flat spectral background, good sharpness, conservation of quasiparticle states, and by no shape dependence on the tip-sample distance. These conditions demonstrate the good quality of the tunneling junction. The spectra show a relatively small gap $\simeq 5$ mV with almost no excitations inside. It is followed by two further peaks, that are seen in both occupied and empty states sides. As we shall describe below, these features corre-

spond to the larger second superconducting gap $\Delta = 7.5$ meV. It exceeds all those reported in the tunneling literature [10–14]. Consequently, the corresponding ratio $2\Delta/k_B T_C = 4.5$ clearly points to strong electron-phonon coupling.

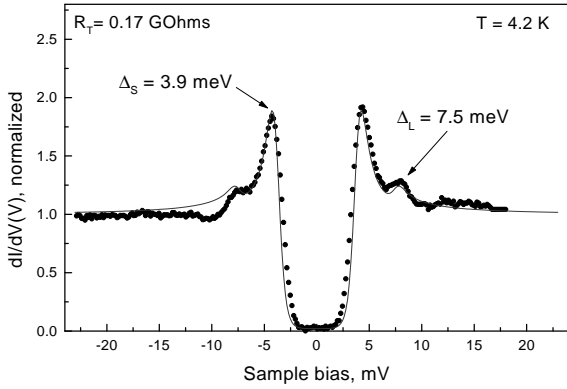


FIG.1 : Double gap structure in local conductance spectra (dots). A small gap $\Delta_S = 3.9$ meV and a large one $\Delta_L = 7.5$ meV exist together. Flat spectral background and zero states at the Fermi energy are characteristic features of such spectra. Solid line: A generalized BCS fit, using Eqs. (1-3), with the parameters $\Gamma = 0$ meV and spectral weights $C_S = 0.94$ and $C_L = 1 - C_S = 0.06$.

An analogous double-gap spectrum was very recently observed in an inverted SIN junction [17] and in an independent point-contact spectroscopy experiment [18]. It has also been shown that both gaps close at the same temperature [17], i.e. the critical temperature T_C of the bulk material. Thus both gaps are intimately related to the superconducting properties of MgB_2 . This behavior is consistent with the theoretical prediction of Liu et al [5] for two gap superconductivity in the clean limit for bulk MgB_2 .

A double gap, such as in Fig.1, is remarkable but could *a priori* originate from different physical scenarios. In the first one, the small gap reflects a proximity superconductivity induced in a thin metallic surface layer. In this case, the observed bump indicates the position of the superconducting gap of the bulk MgB_2 [16]. In the second scenario the small gap is due to a weakened superconductivity on the very surface. Then two tunneling contributions may exist: one corresponding to tunneling to the weakly superconducting surface and another to the bulk MgB_2 directly. Again, the feature at 7.5 meV determines the energy of the bulk gap.

A third and simpler interpretation is the intrinsic double gap scenario for the bulk superconductivity in MgB_2 as predicted for the clean limit [5]. It originates from the existence of two different sheets of the Fermi surface, quasi-2D cylinders and a three-dimensional tubular network, and from a very particular anisotropic phonon spectrum. This results in a strong electron-phonon coupling with the quasi-2D bands and a much weaker coupling to the 3D band.

Finally, two distinct and observable superconducting gaps appear in the quasiparticle spectrum, one larger and the other smaller than the BCS value. The effect is very sensitive to impurities, and vanishes in the dirty limit in which just one gap exists. Taking into account the very short coherence length $\xi \leq 50$ Å [19], it is quite possible that both clean and dirty limit conditions may be found on the surface of such a granular sample.

Further tunneling data are presented in Fig.2 as strong evidence in favor of two gap superconductivity. Here the conductance spectra, selected from different locations of the same sample, clearly show double-peak structures of various relative amplitudes. Remarkably, the energy positions of the gaps remain fixed, which is difficult to explain in terms of a proximity effect. Indeed, in the latter case the DOS is a complicated function of the SN sandwich parameters (interface transparency, metallic layer thickness, diffusion coefficient, etc.) and may be calculated using Usadel's equations [20]. In particular, both the apparent amplitudes of the peaks and their energy positions (especially those of the small induced gap) are very sensitive to any change of the SN sandwich parameters. This is evidently not the case in Fig.2 (a), in which the relative amplitude of the gaps changes markedly, but their positions remain robust, clearly revealing two characteristic energies

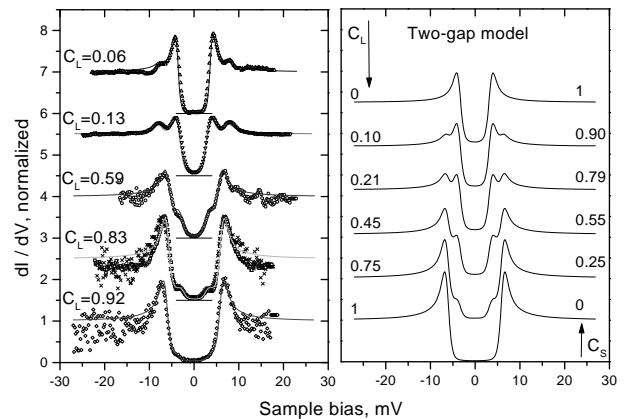


FIG.2. (a) Tunneling conductance spectra ($T = 4.2$ K) normalized to unity and shifted for clarity (horizontal bars indicate zero conductance). The values of the gap widths (Δ_S and Δ_L) are fixed but the relative strength of the peaks vary. The spectra can be fitted by only adjusting the coefficient C_L the weight-factor of the large gap to the total density of states. The spectrum $C_L = 0.13$ was obtained in inverted SIN case [17]. (b) Theoretical curves for the two-gap model, Eqs. (1-3), with different values for the tunneling probabilities C_L , $C_S = 1 - C_L$. The case $C_L = 1$ gives the usual BCS density of states with gap width Δ_L , while $C_L = 0$ ($C_S = 1$) represents the BCS case with gap width Δ_S .

The double-gap superconductivity explains naturally the above observations. While the peak positions are fixed, i.e. corresponding to two energy gaps, the spectral weight of each reflects the probability of tunneling to different electronic bands (2D and 3D). Indeed, in powder based samples the orientation of grains with respect to the tunneling cone varies, as do the respective tunneling probabilities, from one location to another. This explains the variation of the relative amplitudes of the coherence peaks from grain to grain. As illustrated in Fig. 2 (b), the double-gap spectra can be generated by a weighted sum of two BCS density of states with coefficients C_L and C_S ($C_L + C_S = 1$) for the large and small gap DOS, respectively :

$$\sigma(V) = C_L \sigma^L(V) + C_S \sigma^S(V), \quad (1)$$

with :

$$\sigma^{L,S}(V) \propto \int_{-\infty}^{+\infty} g(\epsilon - eV) \rho^{L,S}(\epsilon) d\epsilon, \quad (2)$$

$$\rho^{L,S}(\epsilon) = \text{Re} \left[\frac{\epsilon - i\Gamma}{\sqrt{(\epsilon - i\Gamma)^2 - \Delta_{L,S}^2}} \right]. \quad (3)$$

Here $g(\epsilon) = -\partial f(\epsilon)/\partial \epsilon$ is the usual thermal broadening function and Γ is Dyne's smoothing parameter.

This simple analysis, Eqs. (1-3), appears sufficient to fit all of the double-gap conductance spectra of Fig. 2 (a) (solid lines in the figure). We obtain statistically, $\Delta_L = 7.5 \pm 0.5$ meV and $\Delta_S = 3.5 \pm 0.4$ meV with the smearing term not exceeding $\Gamma = 0.2$ meV. The double structure and other DOS features (zero bias conductance, spectral background, etc.) are perfectly reproduced by the theoretical function for different values of C_L . Even for the bottom spectrum in Fig.2 (a), for which the existence of the inner gap is not so evident, it was necessary to include both gap contributions.

The double gap structure represents only a very small fraction of the acquired data over the surface. The STS technique allows to systematically explore different regions showing a variety of quasiparticle spectra. A complete $I(V)$ spectrum is acquired locally at each pixel (x, y) of the STM image, so that a perfect correspondence between topographic and spectroscopic information is achieved. Moreover, a huge number of tunneling spectra are acquired (up to 65536 $I(V)$ curves per image) allowing a significant statistics. The raw $I(V)$ curves are numerically differentiated and presented either as a series of tunneling conductance maps $dI/dV(V_i, x, y)$, at a chosen bias V_i , or as tunneling conductance spectra $dI/dV(V, x_i, y_i)$ measured in particular locations (x_i, y_i) . More details concerning our STS experimental setup can be found in [8].

In Fig.3 we give an example of such an STS measurement. Image (a) is the topography, acquired simultaneously, of the surface (220×220 nm²) showing relatively flat terraces, with a roughness of about 1-3 nm separated by steps 1-20 nm high. It does happen that the tip jumps from one region to another due to the surface roughness on a larger scale. A single occurrence of this is indicated in (a) by the arrow.

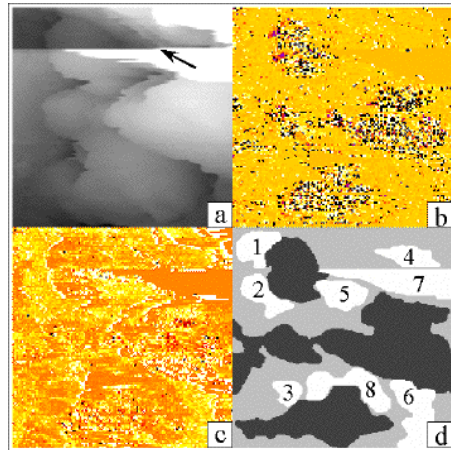


FIG. 3. Complete DOS mapping of a $220\text{nm} \times 220\text{nm}$ area of a chosen MgB_2 grain. (a) Topographic image acquired in the constant current mode (sample bias $V = -18$ mV, $I = 80$ pA). Flat regions are resolved. Black arrow indicates a tip jump during a scan. (b) Conductance map of the same area at $V = -15$ mV. (c) Conductance map at $V = +5$ mV. Bright and dark zones respectively indicate high and low conductance zones. (d) In black: ‘contaminated’ regions (as found from (b)); in white: selected regions (numbered from 1 to 8) described in the text.

In Fig.3 (b) we show the tunneling conductance map at $V = -15$ mV proving that the DOS is spatially inhomogeneous. Regions in which high-quality tunneling conditions are not met (the current is noisier, probably due to the surface contamination) are in black in Fig.3 (d). Of particular interest is the conductance map for $V = +5$ mV, i.e. at an energy close to the expected superconducting gap edge, Fig.3 (c). In this map, bright and dark zones reveal the co-existing regions with high and low conductances. Comparing the topographic image (a) with the two conductance maps (b) and (c), we can easily select the most ‘significant’ regions in which noiseless tunneling conditions are achieved on a relatively flat surface. Such regions, of a typical size of 10-30 nm, are colored in white and numbered from 1 to 8 in Fig.3 (d). As a simple approach, the spectra are averaged over each selected region and the results are plotted in Fig.4.

The conductance spectra from the regions 1 and 2 are quite similar and both spectra present a smoothed reduced gap of about 2.5 meV. The ratio $2\Delta/k_B T_C = 1.48$ ($T_C = 39$ K for the bulk) is less than two times smaller than the weak coupling BCS ratio. Such spectra originate

either from the weakened T_C on the surface (due to the local surface degradation) or from a proximity induced gap. The conductance at zero-bias is far from zero and these spectra show a strong smearing term $\Gamma = 0.3 \Delta$. Contrary to what was suggested in [11], Γ does not reflect the properties of the bulk MgB_2 since it varies spatially, and even vanishes in other regions. This type of spectrum was also observed by Sharoni et al. [13] and explained in terms of the proximity effect.

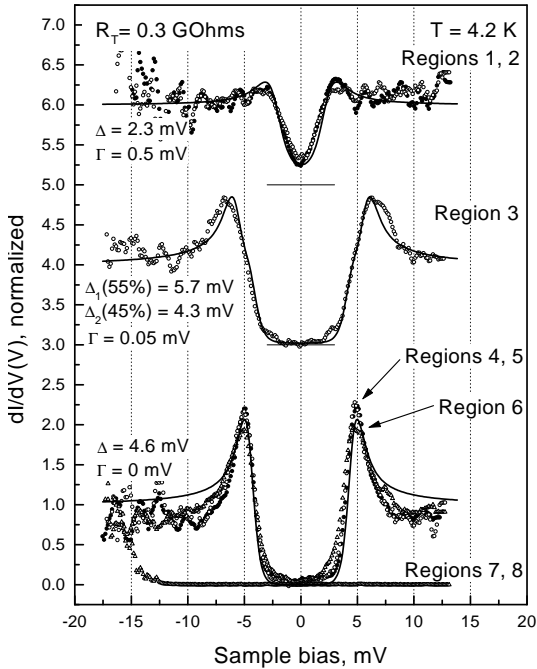


FIG.4. Normalized tunneling conductance spectra corresponding to the regions 1-8. The data points are shifted for clarity (horizontal bars indicate zero tunneling conductance). The spectra in the regions 1-2 present a small gap $\Delta = 2.5$ meV. These smoother spectra are fit (solid line) with a large Γ (0.3Δ). In region 3, the gap width varies spatially, giving a smeared averaged characteristic, well fit (solid line) by two gaps of 4.3 mV and 5.7 mV and $\Gamma \ll \Delta$. In the regions 4-6 the spectra have a BCS shape with a single gap. The theoretical fit (solid line) with $\Delta = 4.6$ meV and $\Gamma = 0$ meV is satisfactory. Regions 7-8: tunneling conductance shows no states, i.e. insulating behavior, in the energy window studied.

The detailed analysis of region 3 (about 20 nm size) shows that two characteristic spectra are present: the first one, about 45% of the area, shows a gap of 4.3 meV, while the second one has a gap of 5.7 meV (about 55%). Thus, the average dI/dV curve in Fig.4, having a small $\Gamma = .05$ meV, has a kink at the small gap energy. Regions 4-6 are the most homogeneous and have the sharpest tunneling spectra with a clear single-gap BCS shape. The coherence peaks are very high and are situated at the same energy, and no states exist inside. Only thermal broadening is needed ($\Gamma = 0$ meV), how-

ever the average gap value $\Delta = 4.6$ meV, is still significantly small, i.e. less than the ideal BCS value of 5.9 meV by 20%. In view of the double gap spectra, as in Figs.1 and 2, this characteristic single gap must correspond to the dirty limit. We conclude that about 99 % of the STS conductance spectra yield a single gap, with a probable reduced T_C , due to proximity effects or the dirty limit cases. Thus, the STS explains why the double gap DOS was not observed in previous tunneling reports.

In conclusion, in this Letter we report the first direct evidence for two superconducting gaps in MgB_2 . These are due to different electron-phonon coupling in the two distinct parts of the Fermi surface, in agreement with the multiple gap model [5]. It is also consistent with the variation in relative spectral weight observed, due to the arbitrary orientation of the tunneling cone to the grains. The additional study of the temperature dependence of the two gaps supports our conclusions [17]. In the proximity effect or lowered surface T_C scenarios, the small gap should close at a lower temperature, while it should survive until 39 K together with the large gap in the double gap picture. No evidence for any large anisotropy of the order parameter nor pair breaking is found in the best spectra reported here. More significantly, the value of the large gap (7.5 ± 0.5 meV) leads to the ratio $2\Delta/k_B T_C = 4.5 \pm 0.3$ indicating the presence of strong electron-phonon coupling. STS performed on granular MgB_2 at $T = 4.2$ K, shows the importance of spatial inhomogeneities in such samples.

This work was supported by the Project ACI “Nanostuctures” of the French Ministry of Research.

-
- [1] J. Nagamatsu et al., Nature **410**, 63 (2001)
 - [2] et al., Phys. Rev. Lett. **86**, 1877 (2001).
 - [3] H. Kotegawa et al., cond-mat/0102334
 - [4] J. Kortus et al., cond-mat/0101446.
 - [5] A. Y Liu et al., cond-mat/0103570.
 - [6] T. Takahashi et al., cond-mat/0103079.
 - [7] S. Tsuda, et al., cond-mat/0104489.
 - [8] T. Cren et al., Eur. Phys. Lett. **54**, 84 (2001).
 - [9] W.L. Macmillan and J.M. Rowell, Phys. Rev. Lett. **14**, 108 (1965).
 - [10] G. Rubio-Bollinger et al., cond-mat/0102242.
 - [11] G. Karapetrov et al., Phys. Rev. Lett. **86**, 4374 (2001).
 - [12] H. Schmidt et al., cond-mat/0102389.
 - [13] A. Sharoni, O. Millo, and I. Felner, cond-mat/0102325.
 - [14] H. Schmidt et al., Phys. Rev. B **63**, 220504(R) (2001).
 - [15] C.T. Chen et al., cond-mat/0104285.
 - [16] W.L. McMillan, Phys. Rev. **175**, 537 (1968).
 - [17] F. Giubileo et al., cond-mat/0105592.
 - [18] P. Szabo et al., cond-mat/0105598.
 - [19] D.K. Finnemore et al., Phys. Rev. Lett. **86**, 2420 (2001).
 - [20] K.D. Usadel, Phys. Rev. Lett. **25**, 505 (1970).